

# COD: A Cooperative Cell Outage Detection Architecture for Self-Organizing Femtocell Networks

Wei Wang, *Student Member, IEEE*, Qing Liao, *Student Member, IEEE*, Qian Zhang, *Fellow, IEEE*

**Abstract**—The vision of Self-Organizing Networks (SON) has been drawing considerable attention as a major axis for the development of future networks. As an essential functionality in SON, cell outage detection is developed to autonomously detect macrocells or femtocells that are inoperative and unable to provide service. Previous cell outage detection approaches have mainly focused on macrocells while the outage issue in the emerging femtocell networks is less discussed. However, due to the two-tier macro-femto network architecture and the small coverage nature of femtocells, it is challenging to enable outage detection functionality in femtocell networks. Based on the observation that spatial correlations among users can be extracted to cope with these challenges, this paper proposes a Cooperative femtocell Outage Detection (COD) architecture which consists of a trigger stage and a detection stage. In the trigger stage, we design a trigger mechanism that leverages correlation information extracted through collaborative filtering to efficiently trigger the detection procedure without inter-cell communications. In the detection stage, to improve detection accuracy, we introduce a sequential cooperative detection rule to process spatially and temporally correlated user statistics. Numerical studies for a variety of femtocell deployments and configurations demonstrate that COD outperforms the existing scheme in both communication overhead and detection accuracy.

**Index Terms**—Femtocell, Self-Organizing Networks, Cell Outage Detection

## I. INTRODUCTION

Self-Organizing Networks (SON) have recently been recognized as an attractive paradigm for the next-generation cellular systems by standardization bodies [1], [2], which enables autonomic features in networks, including self-configuration, self-optimization and self-healing [3], [4]. In the self-healing mechanism, cell outage detection is considered to be one of the fundamental functionalities, which aims to autonomously detect cells in an *outage* state, i.e., cells that are inoperable and cannot provide any service due to hardware failures, software failures or even misconfigurations [2]. Cell outage often results in decreased capacity and coverage gap. Such degraded performance leads to high user churn rate and operational expenditures [5]. However, detecting outaged cells is non-trivial. The outaged cells cannot be detected by Operations Support System (OSS) when the detection systems of the outaged cells malfunction [6]. In addition, it is difficult for the cellular system management functions to detect outaged

cells directly when the outage is caused by misconfigurations. Identifying these outaged cells usually requires unplanned site visits and usually takes hours or even days [5]. To reduce manual costs and detection delay, the cell outage detection function is proposed in [2] to automatically identify the outaged cells by users' performance statistics analysis.

The 3GPP standard [2] defines the essential steps to realize cell outage detection function: i) performance statistics are monitored continuously, and ii) an appropriate self-healing process is triggered if the monitored parameters meet the cell outage detection condition. Research community explores different approaches to realize the functions and fulfil the requirements determined in the standard. Most, if not all, previous cell outage detection approaches have focused on macrocells [7]–[9]. However, traditional macrocell networks are likely to be supplemented with smaller femtocells deployed within homes and enterprise environments in the next-generation cellular networks [10], [11], where outage occurs more frequently because of inappropriate indoor human interactions and unplanned deployments of large numbers of femto access points (FAPs). Unfortunately, when applied to femtocell networks, existing macrocell outage detection works fall short due to the distinct features of femtocell networks. The distinct features of femtocell networks that differ from macrocell networks are described as follows.

- **Dense deployments.** Since there are normally tens or hundreds of femtocells deployed within a macrocell, the number of femtocells is much larger compared with macrocells. The centralized statistics analysis adopted by macrocell outage detection approaches [7] [8] will involve high communication overhead if applied directly in femtocell networks, which will degrade the femtocell service.
- **Vertical handover.** Femtocell users can vertically handover between femtocell and macrocell. However, this vertical handover issue is not considered in the existing macrocell outage detection approaches [7], [8]. In the two-tier femto-macro cellular networks, when a femtocell outage occurs, its users may handover to macrocell and be unaware of the outage. This can be misleading in the user statistics analysis.
- **Sparse user statistics.** Unlike macrocell with large coverage, small scale indoor femtocell usually only supports a few active users (typically 1 to 4 active mobile phones in a residential setting [12]). Macrocell approaches [7],

W. Wang, Q. Liao and Q. Zhang are with the Department of Computer Science and Engineering, Hong Kong University of Science and Technology, Hong Kong. e-mail: {gswwang, qnature, qianzh}@cse.ust.hk.

[8], which are based on user statistics within one cell, however, fall inaccurate due to the sparsity of user statistics with high uncertainty caused by severe indoor shadow fading. In the worst case, femtocell with small coverage may have no active users in certain time slots, leading to the failure of these algorithms.

To overcome the aforementioned challenges in femtocell networks, we propose an efficient detection architecture, referred to as *COD* (Cooperative femtocell **O**utage **D**etection), which consists of an intra-cell trigger stage and an inter-cell detection stage. The core idea of this architecture includes the following considerations: 1) To reduce communication overhead, the trigger procedure runs on each FAP in a distributed manner without any inter-cell communications. We design a low cost mechanism to trigger the detection for possible outage femtocell via long term passive monitoring of users' *Reference Signal Received Power* (RSRP) statistics. The RSRP statistics are user's basic physical layer measurements on the linear average of the downlink reference signals across the channel bandwidth [13]. 2) The trigger decisions are based on spatial correlations among users' RSRP statistics, rather than disconnected devices [14], [15] or neighbor list [7] as in traditional approaches. The RSRP statistics correlations are leveraged to distinguish the vertical handover case and the outage case. 3) To cope with the data sparsity issue, a detection rule enables neighboring femtocells to cooperatively detect outaged femtocells over a certain period of time, so as to expand the statistics over the space domain and the time domain to obtain enough information. A data fusion rule is used to process the statistics to make a final decision.

According to the above three guidelines, the key problems behind this architecture are *how to extract correlations of intra-cell RSRP statistics in space domain* and *how to extract correlations of inter-cell RSRP statistics in space and time domains*. To tackle these two problems, We propose an efficient trigger mechanism and a cooperative detection rule, respectively. In the trigger stage, each FAP predicts the current normal RSRP statistics of its neighboring cells based on the notion of collaborative filtering [16]. To leverage collaborative filtering in RSRP prediction, we propose an efficient algorithm with convergence guarantee and provable error bound. The trigger decision is made based on the comparison between the predicted statistics and real statistics. In the detection stage, statistics within a geographical area, referred to as *cooperation range*, are processed at the macrocell base station (MBS) via the sequential detection model [17]. Based on this model, we exploit the spatial characteristics of the statistics to derive the minimal time needed to make a final decision.

To the best of our knowledge, this paper is the first work to explore the outage detection problem in the context of femtocell networks. The main contributions of this work can be summarized as follows:

- This paper proposes a correlation based outage detection architecture for the two-tier femtocell networks. In particular, we consider the challenge caused by the salient features of femtocell networks, i.e., dense deployments, vertical handover, and sparse user statistics. This archi-

ture can be used as a general framework for designing femtocell outage detection schemes.

- A distributed trigger mechanism with provable error bound and convergence guarantee is designed to reduce the communication overhead and to address the vertical handover issue. The trigger mechanism leverages collaborative filtering to exploit the spatial correlations of RSRP statistics. The extracted spatial correlations enable the trigger mechanism to make a trigger decision without any inter-cell communication overhead. To leverage collaborative filtering in RSRP prediction, we also propose an efficient algorithm with guaranteed convergence and provable error bound.
- A cooperative detection rule is proposed to cope with the data sparsity issue by extracting both the spatial and temporal correlations of RSRP statistics over multiple femtocells. In particular, we take sequential hypothesis testing as data processing rule, based on which we identify the impacts of the cooperation range and the user density on detection performance by deriving closed-form expressions. Analytical results show that the expected detection delay is inversely proportional to the user density and the cooperation area, and is independent of the FAP's transmission power.
- We conduct extensive numerical studies, and the evaluation results show that the proposed approach outperforms the conventional method in terms of communication cost as well as detection accuracy.

The rest of the paper is organized as follows. Related works are reviewed in Section II. Section III describes the system model. Section IV illustrates the rationale of the proposed COD architecture. Section V introduces the trigger mechanism in COD, and analyzes its convergence property and error bound. Section VI formulates the cooperative outage detection problem in COD as a sequential hypothesis testing problem and derives analytical results. Numerical results are presented in Section VII. Finally, Section VIII concludes the paper.

## II. RELATED WORK

SON functions are defined in 3GPP standards [1], [2] to reduce capital and operational expenses by bringing self-configuration, self-optimization, and self-healing abilities to cellular systems [18], [19]. Many existing works have focused on self-configuration and self-optimization [20]–[22]. General issues in self-configuration and self-optimization in heterogeneous cellular networks are studied in [20]. Inter-cell interference mitigation approaches are proposed in [21], [22] as a use case in self-optimization function. Recently, self-healing issue in cellular networks has also been studied in the research community [9], [23]–[26]. Most of these studies have devoted to cell outage compensation [24]–[26]. Cell outage compensation aims at mitigating the degradation of coverage, capacity and service quality caused by cell outage. Amirijoo et al. [24] formulate the macrocell outage compensation as an optimization problem to maximize coverage given the constraints on quality defined in terms of cell-edge user throughput. Xia et al. [25] propose a genetic algorithm based mechanism to

minimize network performance degradation. Different from [24], [25], Wang et al. [26] focus on self-healing problem in femtocell networks, and propose a local cooperative architecture to allow more femtocells to assist the recovery process of an outaged femtocell. In this paper, we have focused on the cell outage detection part of self-healing function. Existing cell outage detection schemes have focused on macrocell [7], [9], [27]. A autonomous clustering algorithm is proposed in [9] to collect RSRP statistics for outage detection. In [7], user's neighbor cell list reports are leveraged to construct a visibility graph, whose topology changes are used to detect outaged macrocells. However, these cell outage detection studies do not consider the distinct features of femtocell networks, and thus cannot be directly applied to femtocell outage detection. Mobility robustness optimization (MRO) [28] is a solution for automatic detection and correction of errors in the mobility configuration, while this paper focuses on the outage that total radio services fail. Minimization of driving test (MDT) technique [27], [29] detects outage by comparing the current measurements with pre-stored measurements that model the normal case. The MDT technique is similar to the benchmark data used in this paper, while the difference is that we extract the spatial correlations based on collaborative filtering to cope with the unique challenges in femtocell networks.

Troubleshooting has been studied in previous works [7], [8], [30]. Khanafer et al. [8] propose a framework to process historical user statistics via offline Bayesian analysis to diagnose the root causes for the cell outage. Based on a similar but enhanced offline analysis model, Wang et al. [30] further study the outage troubleshooting problem in the context of femtocell networks. These works focus on offline analysis of the root causes after an outage has been detected, while we emphasize the online detection of the outaged cell.

In wireless LANs, there have been a lot of studies on node failure and faults detection problems [14], [15]. [15] is the first study on fault detection and diagnosis in the IEEE 802.11 infrastructure wireless networks. In [15], the *client conduit* protocol is proposed to allow clients to cooperatively identify the root cause of disconnection issues. A fault management system is designed in [14] to automatically detect fault nodes and troubleshoot network problems, in which the detection procedure is triggered only when a client is disconnected from AP. However, these outage or fault detection approaches cannot be applied to the femtocell outage detection scenario due to the unique challenges listed in Section I.

In cognitive radio networks, primary user detection [31], [32] is also related to our work. These works focus on detecting the signals of primary users by spectrum sensing. The fundamental differences between these works and ours are twofold. First, the issues caused by the two-tier architecture of femtocells are not involved in these works. Second, the communication overhead is more strictly constrained in femtocell outage detection since femtocell should guarantee quality of service for the users in the first place.

### III. SYSTEM MODEL

In this section, we introduce the network model, the user model and the channel model.

#### A. Network Model

We consider a typical two-tier femtocell network architecture where a set of femtocells  $\mathcal{F} = \{1, \dots, F\}$  are overlaid on a macrocell. Femtocell  $f$  operates under the FAP  $f$ . A femtocell experiences outage with certain probability in the process of operation. The outaged FAP cannot transmit or receive any signal. We assume that the coarse location information of FAPs can be obtained by the MBS. FAPs transmit reference signals periodically in the downlink. The reference signals, which facilitate user's channel measurements (e.g., the RSRP measurement), are sent back to the FAPs as feedback messages.

#### B. User Model

The locations of the users are unknown. The users transmit or receive data from their associated FAPs, and periodically report the RSRP statistics of all neighboring cells to their associated FAPs, providing guidance in handover and cell reselection decisions. We assume that the users in an area  $A$  follow a Poisson point process with density  $\rho$ , i.e.,  $n_A \sim Poi(n; \rho|A|)$ , where  $n_A$  is the number of users within the area  $A$ .

#### C. Channel Model

The channel gains of a user  $u$  to an FAP  $f$  are determined based on the model described in [33]:

$$h = \left(\frac{d_o}{d_{u,f}}\right)^a e^{X_{u,f}} e^{Y_{u,f}}, \quad (1)$$

where  $d_o$  is the reference distance (e.g., 1 m),  $d_{u,f}$  the distance between the FAP  $f$  to the user  $u$ , and  $a$  the path loss exponent.  $e^{X_{u,f}}$  and  $e^{Y_{u,f}}$  are shadow fading factor and multi-path fading factor, respectively. The shadow fading follows a Gaussian distribution described by  $X_{u,f} \sim \mathcal{N}(0, \sigma)$ ,  $\forall u, f$ . The multi-path fading is modeled by Rayleigh fading with zero mean, and thus  $\mathbb{E}[e^{Y_{u,f}}] = 0$ .

Shadow fading effects are assumed to be independent over time. With this assumption, the RSRP statistics of a user are independent random variables. Note that all RSRP statistics of a user can be characterized by Eq. (1). As such, the RSRP statistics at a certain user  $u$  are independent and identically distributed (i.i.d.), and thus can be approximated as a Gaussian distribution using the *Central Limit Theorem* (CLT). Then, the distribution can be given as [34]:

$$r_u \sim \begin{cases} \mathcal{N}(N_o, \frac{N_o^2}{M}) & \mathcal{H}_0 \\ \mathcal{N}(P_u + N_o, \frac{(P_u + N_o)^2}{M}) & \mathcal{H}_1 \end{cases} \quad (2)$$

where  $r_u$  is user  $u$ 's RSRP statistics,  $P_u$  the received signal strength at user  $u$ ,  $N_o$  the noise power, and  $M$  the number of signal samples, e.g.,  $5 \times 10^3$  /ms for 5 MHz band.  $\mathcal{H}_0$  stands for the outage case and  $\mathcal{H}_1$  for the normal case.

### IV. RATIONALE OF THE COD ARCHITECTURE

In this section, we first use a motivational example to illustrate the requirements of femtocell outage detection and our observation. Then, we propose the COD architecture.

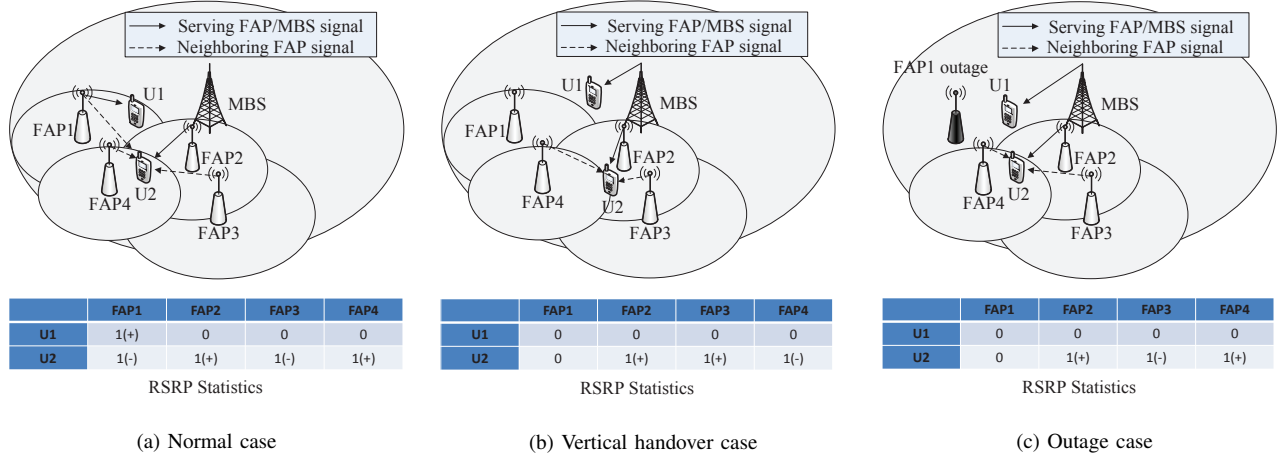


Fig. 1: Cases in femtocell outage detection

### A. Requirements of Femtocell Outage Detection

Due to the unique features of femtocell networks, the following requirements need to be imposed when designing a femtocell outage detection architecture.

First, the communication overhead should be minimized to preserve the capacity of the femtocells. This can be achieved by: 1) designing a distributed trigger mechanism that involves much less communication overhead compared with the detection stage, and 2) minimizing the detection time (i.e., detection delay) of the detection stage.

Second, the effectiveness of the outage detection should be guaranteed even in the event of vertical handover. Fig. 1 illustrates the vertical handover issue in the two-tier femto-macro architecture. In the normal case (Fig. 1(a)), all femtocells operate normally and the user U1 is associated with the femtocell FAP1. Then, U1 vertically handovers to the MBS, which is caused by the movement of U1 (Fig. 1(b)) or the outage of FAP1 (Fig. 1(c)). Unfortunately, many existing approaches cannot differentiate the outage case (Fig. 1(c)) from the vertical handover case (Fig. 1(b)). In wireless LAN diagnosis or fault detection, the detection procedure is usually triggered by disconnected users [14], [15], which is not applicable in femtocell outage detection since users can handover to macrocell when there is no available femtocell around (e.g., Fig. 1(c)). Neighbor list based approaches [7], [35] are proposed to detect outages by looking at the changes in the network topology. The core idea of neighbor list based approaches is to construct a visibility graph based on UEs' reports about neighbor cells whose signals can be heard by the UEs. As listed in the tables in Fig. 1(b) and Fig. 1(c), the neighbor lists of UEs in both cases are the same. As such, the visibility graphs constructed based on UEs' neighbor lists are identical in these two cases, and thus cannot distinguish the outage case from the vertical handover case. Therefore, a trigger mechanism that can differentiate between these two cases is required.

Another unique feature of femtocell is that, the indoor femtocell supports much fewer users compared with the macrocell. Since severe indoor shadow fading results in the fluctuation

of user statistics, analysis based on the sparse user statistics may lead to inaccurate results. To design a robust detection rule, the accuracy should be guaranteed even when femtocells have very few users.

### B. Observation

To design a femtocell outage detection architecture that achieves the aforementioned requirements, we further investigate the spatio-temporal correlations in RSRP statistics. In Fig. 1, U2 keeps moving in all the three cases, while U1 remains in the same location in the normal case and the outage case but moves away from FAP1 in the vertical handover case. The tables in Fig. 1 show the corresponding RSRP statistics, which are classified into three levels: 1(+) for strong received signal from a certain FAP, 1(-) for weak received signals, and 0 for no received signal. Comparing Fig. 1(a) and Fig. 1(c), U2's RSRP statistics from FAP2-FAP4 are the same while the RSRP statistics from FAP1 are different. A previous study [36] shows that users in close proximity have similar signal statistics, and the estimation of location similarity is more accurate when there are more FAPs nearby. Therefore, we can infer that the locations of U2 in Fig. 1(a) and Fig. 1(c) are probably close, and thus the RSRP from FAP1 should be similar in the two figures if FAP1 is normal in Fig. 1(c). Thus, the difference between RSRP statistics from FAP1 in the two figures indicates that FAP1 may be experiencing outage in Fig. 1(c). On the other hand, comparing Fig. 1(a) and Fig. 1(b), the locations of U2 are considered to be quite different since the U2's RSRP statistics from FAP2-FAP4 in both cases have weak correlations. Therefore, even though the RSRP statistics from FAP1 are very different in the two cases, we cannot infer whether FAP1 is experiencing outage or not. Based on the above analysis, we observe that the UE vicinity relations that lie in the RSRP statistics can be used to enhance outage detection. To achieve this goal, an FAP can check the states of neighboring FAPs by comparing current statistics with historical statistics in normal cases. Note that the scenario discussed above is only a toy example to illustrate that it is possible to leverage user statistics across different

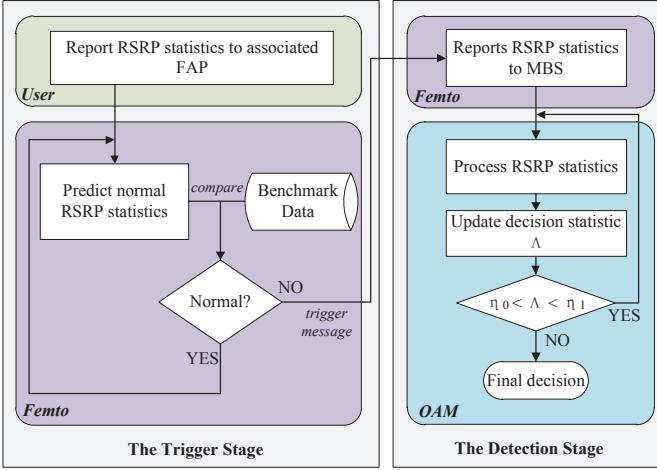


Fig. 2: Architecture overview

femtocells to detect outages. While the topology is simple in this example, the observation is applicable to general cases of typical two-tier femto-macro networks.

Based on this observation, we can tackle the vertical handover issue and enable the distributed trigger mechanism. In the trigger mechanism, each femtocell monitors the state of its neighboring femtocells based on correlations between current RSRP statistics and historical RSRP statistics reported by the users. Moreover, multiple femtocells can cooperatively process RSRP statistics by further exploiting the correlations over a period of time to cope with the user sparsity issue.

### C. COD Architecture Overview

The goal of COD is to detect outaged femtocells accurately and efficiently by meeting the requirements discussed in Section IV-A. To achieve this goal, two stages are involved: a distributed trigger stage with no inter-cell communications, and a cooperative detection stage with high accuracy and little delay. In the trigger stage, each FAP collects the user-reported RSRP statistics and sends the MBS a trigger message if current statistics are abnormal. Then, the MBS initiates the detection stage and makes a final decision based on RSRP statistics collected from multiple FAPs within the cooperation range.

Fig. 2 illustrates the COD architecture. Before the trigger stage, each FAP stores a copy of *benchmark data* beforehand, which is collected when all FAPs are normal. Benchmark data contains the RSRP statistics from all neighboring FAPs in the form of a matrix  $\mathbf{R}$ , where element  $R_{u,f}$  in  $\mathbf{R}$  is the RSRP of user  $u$  from FAP  $f$ . In self-organizing femtocell networks, the initial benchmark data can be collected at the self-configuration phase. Then, the benchmark data is updated by adding newly reported RSRPs and removing the outdated RSRPs to maintain a constant size.

In the trigger stage, each FAP runs the trigger algorithm to monitor the states of neighboring femtocells by checking the reported RSRP statistics from its associated users. To check whether the RSRP statistics are normal or not, the FAP predicts the expected normal RSRP statistics based on the benchmark data via collaborative filtering. As for an FAP  $i$ , if the RSRP

statistics from a neighboring FAP  $f$  deviate from the predicted normal statistics, then FAP  $i$  will send a trigger message to the MBS to trigger the detection stage to further decide whether the FAP  $f$  is experiencing outage. Otherwise, FAP  $i$  updates its benchmark data with the RSRPs reported in this round and continues monitoring FAP  $f$  in next round.

In the detection stage, all the FAPs within the cooperation range report the statistics collected in trigger stage to the MBS periodically until the MBS collects enough information to make a final decision. In each iteration, based on the newly reported RSRP statistics, the MBS processes the statistics via data fusion to update decision statistic, and compares it with pre-computed thresholds (i.e.  $\eta_0$  and  $\eta_1$ ), until it is qualified to make a final decision. The thresholds are computed to guarantee the pre-defined false alarm and misdetection rates. If the decision statistic is below the lower threshold (i.e.  $\eta_0$ ), the MBS makes a final decision that FAP  $f$  is experiencing outage. If the decision statistic is above the higher threshold (i.e.  $\eta_1$ ), the MBS decides that FAP  $f$  is normal. Otherwise, the MBS continues to take another round and accumulates more RSRP statistics.

## V. COLLABORATIVE FILTERING-BASED TRIGGER MECHANISM

In this section, we propose a distributed trigger mechanism based on collaborative filtering to make a trigger decision without any inter-cell communication overhead. Then, we analyze the error bound and convergence properties of the proposed mechanism.

### A. Trigger Mechanism

The trigger stage contains two steps, namely, the normal RSRP statistics prediction and the trigger decision, as illustrated in Fig. 2. To predict normal RSRP statistics, we leverage the notion of collaborative filtering to explore the correlations among the femtocell users. Collaborative filtering is originally used in recommendation systems to compare a user's flavor to some reference users' flavors based on their rated items, so as to predict the rating of that user on a certain item. Treating users as rows and items as columns, the ratings form a matrix. Then, collaborative filtering aims to reconstruct a matrix with missing entries by exploiting correlations across different rows. In the trigger mechanism, we consider the femtocell users as users in a recommendation system, the FAPs as items, RSRP statistics as ratings and the benchmark data as the flavor data of reference users. Similar to the recommendation systems, we leverage collaborative filtering to predict the RSRP statistic from a target FAP based on the benchmark data matrix. In contrast to neighbor list based approach, we exploit the fine-grained RSRP values instead of cell-level visibility information. The fine-grained RSRP values contain the vicinity relations among UEs, which can be used to assist outage detection (e.g., vicinity relation can help differentiate the outage case from the vertical handover case as shown in Fig. 1). Note that different from recommendation systems, we consider the RSRPs of a user at different times as separate rows because the same user can have different RSRPs

at different times and locations. Since the benchmark data is collected in normal cases, the predicted RSRP statistic is the expected normal RSRP statistic. If the predicted RSRP statistic and the collected RSRP statistic are significantly different, the target FAP is very likely in an outaged state. Based on this intuition, we design a trigger mechanism as follows.

1) *Normal RSRP Statistics Prediction*: To make a trigger decision, the expected normal RSRP  $r_{u,f}$  of a user  $u$  from the target FAP  $f$  needs to be estimated. The first step is to leverage collaborative filtering to profile users and FAPs by exploiting correlations among them. *Matrix factorization* (MF), which decomposes a matrix as a product of two low-rank latent matrices, is one of the most popular techniques for collaborative filtering with attractive accuracy and scalability [37]. We exploit the correlations of RSRP statistics via MF as follows.

Suppose that the user  $u$  is associated with the FAP  $b$  and  $b$  needs check whether a neighboring FAP  $f$  is normal based on  $r_{u,f}$ . The RSRP statistics of  $u$  from all FAP  $b$ 's neighboring FAPs are denoted as  $\mathbf{r}^u \in \mathbb{R}^{1 \times m}$ , and the benchmark data matrix stored in FAP  $b$  is denoted as  $\mathbf{R}^b \in \mathbb{R}^{(n-1) \times m}$ . Let  $\hat{\mathbf{R}} = \begin{bmatrix} \mathbf{r}^u \\ \mathbf{R}^b \end{bmatrix}$ . Via MF, the RSRP matrix  $\hat{\mathbf{R}}$  is transformed into a low-rank matrix  $\mathbf{U} \in \mathbb{R}^{n \times d}$  representing user's latent profile and another low-rank matrix  $\mathbf{V} \in \mathbb{R}^{m \times d}$  representing FAP's latent profile, where  $d \in \mathbb{N}$  is smaller than  $m, n$ .  $\mathbf{U}$  and  $\mathbf{V}$  are computed as follows.

$$\min_{\mathbf{U}, \mathbf{V}} \left\| \left( \hat{\mathbf{R}} - \mathbf{U}\mathbf{V}^\top \right) \odot \mathbf{I} \right\|_F^2, \quad (3)$$

where  $\| \cdot \|_F$  is the Frobenius norm, and  $\odot$  signifies the element-wise multiplication.  $\mathbf{I}$  is the index matrix to indicate the expected normal RSRP  $\hat{r}_{u,f} \in \mathbb{R}$  that we want to predict by setting the corresponding element in  $\mathbf{I}$ , e.g.,  $I_{1,f}$ , as 0 while leaving all other elements in  $\mathbf{I}$  as 1. We can eliminate  $\mathbf{I}$  by replacing the original value of  $r_{u,f}$  with "Any", where  $x - \text{Any} = 0, \forall x \in \mathbb{R}$ .

However, (3) does not consider the intrinsic geographical structure of femtocells. To remedy this problem, our observation is that the links between a receiver and nearby transmitters experiences similar multipath environments [38], which implies that the nearby FAPs have similar latent profiles. To exploit the geographical structure of femtocells, we leverage the *graph regularized nonnegative MF* (GNMF) [39]. The basic assumption in GNMF is that data points reside on the surface of a manifold that lies in a low-dimensional space, that is, if two data points are close enough in high-dimensional space (i.e., RSRP statistics) they are still close in low-dimensional space (i.e., the FAP's latent profile  $\mathbf{V}$ ). Specifically, GNMF constructs an adjacent graph  $\mathbf{G}$  to represent the local geographical structure of users. In  $\mathbf{G}$ , each node associates an FAP and an edge is established between two nodes if one node belongs to the  $k$  nearest neighbors of another. The node distance is measured by the Euclidean distance between FAPs' latent profiles  $\{\mathbf{V}_f : \forall f\}$ . Based on  $\mathbf{G}$ , we can build an adjacent matrix  $\mathbf{W}$  as follows:

$$w_{ij} = \begin{cases} 1, & f_j \in N_k(f_i) \\ 0, & \text{otherwise} \end{cases} \quad (4)$$

where  $w_{ij}$  is an element in  $\mathbf{W}$  and  $N_k(f_i)$  denotes the  $k$  nearest neighbors of the FAP  $f_i$ . The value of  $k$  is usually set to be a relatively small number as only very close FAPs can maintain vicinity in lower dimension (latent profiles) [40]. However, it is still an open problem in the matrix factorization literature to obtain the optimal value of  $k$ . In our simulations, we empirically set  $k$  to 5, which demonstrates good performance in most cases. To preserve the geographical structure of FAPs, the objective is to minimize

$$\sum_{i=1}^n \sum_{j=1}^n \|\mathbf{V}_i - \mathbf{V}_j\|_2^2 W_{ij} = \text{tr}(\mathbf{V}^\top \mathbf{L} \mathbf{V}) \quad (5)$$

where  $\mathbf{L} = \mathbf{D} - \mathbf{W}$  is the Laplacian matrix of  $\mathbf{G}$ , where  $\mathbf{D}$  is a diagonal matrix defined by  $D_{jj} = \sum_l w_{jl}$ , and  $\text{tr}(\cdot)$  signifies the trace operator over a symmetric matrix. Considering (3) and (5) together, we arrive at the objective of GNMF:

$$\min_{\mathbf{U}, \mathbf{V}} \left\| \left( \hat{\mathbf{R}} - \mathbf{U}\mathbf{V}^\top \right) \right\|_F^2 + \lambda \text{tr}(\mathbf{V}^\top \mathbf{L} \mathbf{V}), \quad (6)$$

where  $\lambda > 0$  is a trade-off parameter over the manifold regularization term.

To solve Problem (6) efficiently, we proposed a rank-one residue approximation algorithm. The main idea is inspired by the well-known rank-one residue iteration [41] and hierarchical alternating least squares [42]. Instead of updating the whole  $\mathbf{U}$  and  $\mathbf{V}$ , we recursively update their columns with the remaining variables fixed. For the  $k$ th column of  $\mathbf{U}$  and  $\mathbf{V}$ , the subproblems are

$$\min_{\mathbf{U}_{\cdot k} \geq 0} \|\mathbf{E}_k - \mathbf{U}_{\cdot k} \mathbf{V}_{\cdot k}^\top\|_F^2 \quad (7)$$

and

$$\min_{\mathbf{V}_{\cdot k} \geq 0} \|\mathbf{E}_k - \mathbf{U}_{\cdot k} \mathbf{V}_{\cdot k}^\top\|_F^2 + \lambda \mathbf{V}_{\cdot k}^\top \mathbf{L} \mathbf{V}_{\cdot k}, \quad (8)$$

where  $\mathbf{E}_k$  denotes the residue of  $\hat{\mathbf{R}}$  after eliminating the  $k$ th column of  $\mathbf{U}$  and  $\mathbf{V}$ , i.e.,  $\mathbf{E}_k = \hat{\mathbf{R}} - \sum_{l \neq k} \mathbf{U}_{\cdot l} \mathbf{V}_{\cdot l}^\top$ .  $\mathbf{U}_{\cdot k}$  and  $\mathbf{V}_{\cdot k}$  denote the  $k$ th columns of  $\mathbf{U}$  and  $\mathbf{V}$ , respectively. The subproblem (8) is derived from the following equation:  $\text{tr}(\mathbf{V}^\top \mathbf{L} \mathbf{V}) = \sum_{k=1}^d \mathbf{V}_{\cdot k}^\top \mathbf{L} \mathbf{V}_{\cdot k}$ .

The following lemma shows that these two subproblems can be efficiently solved.

**Lemma 1.** *The subproblems (7) and (8) can be solved by updating the columns of  $\mathbf{U}$  and  $\mathbf{V}$  according to the following rules:*

$$\mathbf{U}_{\cdot k} = \frac{\prod_+(\mathbf{E}_k \mathbf{V}_{\cdot k})}{\|\mathbf{V}_{\cdot k}\|_2^2}, \quad (9)$$

$$\mathbf{V}_{\cdot k} = \prod_+ \left( (\|\mathbf{U}_{\cdot k}\|_2^2 I + \lambda \mathbf{L})^{-1} \mathbf{E}_k^\top \mathbf{U}_{\cdot k} \right), \quad (10)$$

where  $\prod_+(\cdot)$  is an element-wise projection that shrinks negative entries to zero.

*Proof.* See Appendix A.  $\square$

Based on the above lemma, we show that the update rules always converge to the optimal solution.

**Theorem 1.** *Updating the columns of  $\mathbf{U}$  and  $\mathbf{V}$  according to (9), (10) converges to the optimal solution of the subproblems (7) and (8).*

*Proof.* See Appendix B.  $\square$

After solving Problem (6), we use the latent profiles  $\mathbf{U}$  and  $\mathbf{V}$  to predict the normal RSRP  $r_{u,f}$ . Note that since  $I_{u,f}$  is set to 0, the value of  $r_{u,f}$  will not affect the computation of  $\mathbf{U}, \mathbf{V}$ . Then, the missing element  $r_{u,f}$  in  $\hat{\mathbf{R}}$  can be predicted by  $\mathbf{U}$  and  $\mathbf{V}$ :

$$\hat{r}_{u,f} = \mathbf{U}_u \mathbf{V}_f^\top. \quad (11)$$

2) *Trigger Decision:* Based on the predicted normal RSRP  $\hat{r}_{u,f}$ , the trigger decision is made according to the maximum likelihood rule. In particular,  $\hat{r}_{u,f}$  is treated as the mean of the normal hypothesis  $\mathcal{H}_1$  as defined in Eq. (2), the noise power  $N_o$  as the mean of the outage hypothesis  $\mathcal{H}_0$ , and the actual current RSRP  $r_{u,f}$  as the test statistic. If the probability of  $r_{u,f}$  under  $\mathcal{H}_0$  is larger than the probability of  $r_{u,f}$  under  $\mathcal{H}_1$ , the detection stage is triggered. Otherwise, FAP runs the trigger procedure over again on the newly arrived RSRP statistics.

### B. Error Bound Analyses for Normal RSRP Prediction

Note that previous error bounds derived for low-rank approximation are only for multi-class rating [43], while the RSRP statistics are continuous variables. Besides, the shadow fading should also be considered in the error analysis. With these considerations, we analyze the error bound for our trigger mechanism as follows.

According to the channel model described by Eq. (1), the RSRP statistics are largely affected by shadow fading. In our analysis, multi-path fading is neglected since a typical femtocell channel bandwidth, e.g., 5 MHz [44], is much larger than coherent bandwidth. We denote the true received signal strength matrix without shadow fading as  $\mathbf{P}$ , whose corresponding RSRP matrix is  $\hat{\mathbf{R}}$ . If the unit of signal strength is dBm, we have  $\hat{\mathbf{R}} = \mathbf{P} + \mathbf{X}$ , where  $\mathbf{X}$  is the shadow fading matrix with each element following Gaussian distribution  $\mathcal{N}(0, \sigma)$ . The approximation error with respect to  $\mathbf{P}$  is defined to be  $\mathcal{E}(\mathbf{P}, \mathbf{UV}^\top) \triangleq \frac{1}{mn} \sum_{i=1}^m \sum_{k=1}^n |\mathbf{P}_{i,k} - \mathbf{U}_{i,k} \mathbf{V}_{i,k}|$ . Then, we derive the upper bound of  $\mathcal{E}(\mathbf{P}, \mathbf{UV}^\top)$  through the following theorem.

**Theorem 2.** *For any received signal strength matrix  $\mathbf{P}$  and shadow fading matrix  $\mathbf{X}$  with each element following Gaussian distribution  $\mathcal{N}(0, \sigma)$ , with probability of at least  $1 - \delta$ , we have*

$$\mathcal{E}(\mathbf{P}, \mathbf{UV}^\top) \leq \sum_{i=1}^m \sum_{k=1}^n \left( \sqrt{\sum_{l=d+1}^{\text{rank}(\hat{\mathbf{R}})} o_l^2 + \sum_{l=1}^d |1 - o_l| V_{i,l} U_{k,l}} \right) + \varepsilon, \quad (12)$$

where  $\varepsilon$  satisfies  $e^{-\frac{\varepsilon^2}{2\sigma^2}} (1 - Q(\varepsilon)) = \delta \frac{1}{mn} / 2$ .

*Proof.* See Appendix C.  $\square$

## VI. SEQUENTIAL COOPERATIVE DETECTION VIA DATA-FUSION

In this section, we first formulate the cooperative detection problem in the detection stage as a sequential hypothesis testing problem. Then, we derive the closed-form expression of

average detection delay by approximating the test statistics. Finally, based on the closed-form expression of average detection delay, we analyze the impacts of several system parameters on the performance of the cooperative outage detection.

### A. Sequential Hypothesis Testing

We assume that the detection for FAP  $f$  is triggered. The vector of test statistics collected in detection round  $t$  is denoted as  $\boldsymbol{\theta}_t = [r_{1t}, \dots, r_{it}, \dots, r_{nt}]^T$ , where  $r_{it}$  is the user  $i$ 's RSRP from  $f$  in detection round  $t$ .  $n_t$  is the number of users within the cooperation range  $R$  centered by the location of  $f$ . As shown in Eq. (2), the RSRP statistics can be approximated as a Gaussian distribution in both normal and outage cases. Thus, our outage detection problem is a binary decision problem for deciding whether hypothesis  $\mathcal{H}_0$  or  $\mathcal{H}_1$  is true, given the test statistics  $\boldsymbol{\theta}$ , where  $\boldsymbol{\theta} = [\boldsymbol{\theta}_1^T, \dots, \boldsymbol{\theta}_t^T, \dots, \boldsymbol{\theta}_T^T]$ .

To solve the binary decision problem, the MBS keeps collecting new test statistics from users until the amount of information and the resulting testing performance are satisfied. To achieve this goal, we take Wald's *Sequential Probability Ratio Test* (SPRT) [17] as the data processing rule to decide the stopping time of making a final decision. The main advantage of SPRT is that it requires the minimal number of test statistics to achieve the same error probability, which is attained at the expense of additional computation. In the sequential decision process, the MBS computes the log likelihood ratio and compares it with two thresholds  $\eta_0$  and  $\eta_1$ . It either settles on one of the two hypothesis, or decides to make another round of statistics collection.

The likelihood ratio in detection round  $t$  is defined by:

$$\lambda_t \triangleq \ln \frac{p(\boldsymbol{\theta}_t | \mathcal{H}_1)}{p(\boldsymbol{\theta}_t | \mathcal{H}_0)}, \quad (13)$$

where  $p(\boldsymbol{\theta}_t | \mathcal{H}_k)$  is the joint probability density function (p.d.f.) of test statistics collected in detection round  $t$  under the hypothesis  $\mathcal{H}_k$  ( $k = 0, 1$ ). Note that test statistics are assumed to be i.i.d. and follow the Gaussian distribution described in Eq. (2). Thus, Eq. (13) can be written as:

$$\lambda_t = \ln \frac{p(r_{1t}, \dots, r_{nt} | \mathcal{H}_1)}{p(r_{1t}, \dots, r_{nt} | \mathcal{H}_0)} = \sum_{i=1}^{n_t} \ln \frac{p(r_{it} | \mathcal{H}_1)}{p(r_{it} | \mathcal{H}_0)}, \quad (14)$$

where  $r_{it}$  is approximated as  $r_{it} \sim \mathcal{N}(\mu_k, \sigma_k)$  under the hypothesis  $\mathcal{H}_k$ , according to the CLT. Note that  $\sigma_0^2 = \frac{N_o^2}{M}$  and  $\sigma_1^2 = \frac{P_u + N_o^2}{M}$ , where  $P_u$  and  $N_o$  are the average received signal power at users and the noise power. Recall that in the detection stage, we leverage user statistics from neighbor femtocells to collaboratively check the status of a femtocell. As such,  $P_u$  is the received signal power emitted from a neighbor femtocell to a user. Normally, a femtocell has small coverage, and thus the signals from an FAP to a user associated to a neighbor or even further FAP are usually very weak. Therefore, the SNR corresponding to the signals from an FAP to neighbor users is very low. In a very low SNR environment, it is reasonable to approximate  $(P_u + N_o)$  as  $N_o$ , and hence  $\sigma_1 \approx \sigma_0$ . Then, Eq. (14) can be expressed as:

$$\lambda_t = \frac{(\mu_1 - \mu_0) \sum_{i=1}^{n_t} r_{it} + \frac{1}{2} n_t (\mu_0^2 - \mu_1^2)}{\sigma_0^2}. \quad (15)$$

The next step is to determine the decision statistic  $\Lambda_T$  in detection round  $T$ .  $\Lambda_T$  is defined to be the joint likelihood ratio of a sequential test statistics  $\theta_1, \dots, \theta_T$ :

$$\Lambda_T \triangleq \ln \frac{p(\theta_1, \dots, \theta_T | \mathcal{H}_1)}{p(\theta_1, \dots, \theta_T | \mathcal{H}_0)}, \quad (16)$$

where  $p(\theta_1, \dots, \theta_T | \mathcal{H}_k)$  is the joint p.d.f. of test statistics under  $\mathcal{H}_k$ . Regarding that the test statistics are Gaussian and i.i.d., we have:

$$\Lambda_T = \sum_{t=1}^T \ln \frac{p(\theta_t | \mathcal{H}_1)}{p(\theta_t | \mathcal{H}_0)} = \sum_{t=1}^T \lambda_t, \quad (17)$$

and based on Eqs. (15) and (17), we further derive  $\Lambda_T$  as follows:

$$\Lambda_T = \frac{(\mu_1 - \mu_0)}{\sigma_0^2} \sum_{t=1}^T \sum_{i_t=1}^{n_t} r_{i_t} + \frac{T n_t}{2\sigma_0^2} (\mu_0^2 - \mu_1^2). \quad (18)$$

The decision of SPRT in detection round  $T$  is based on the following rules [17]:

$$\begin{cases} \Lambda_T \geq \eta_1 & \Rightarrow \text{accept } \mathcal{H}_1 \\ \Lambda_T \leq \eta_0 & \Rightarrow \text{accept } \mathcal{H}_0 \\ \eta_0 < \Lambda_T < \eta_1 & \Rightarrow \text{take another detection round,} \end{cases} \quad (19)$$

where  $\eta_1$  and  $\eta_0$  are the detection thresholds, which are determined by the predefined values of desired false alarm rate  $\alpha$  and misdetection rate  $\beta$ . However, the outage detection problem is opposite to the detection problem described in [17] in the sense of misdetection rate and false alarm rate, since  $\mathcal{H}_0$  is hypothesis for outage occurrence while  $\mathcal{H}_1$  for event occurrence in [17]. Thus, the detection thresholds are given by:

$$\eta_1 = \ln \frac{1-\alpha}{\beta} \quad \text{and} \quad \eta_0 = \ln \frac{\alpha}{1-\beta}. \quad (20)$$

where  $\alpha$  and  $\beta$  are the desired false alarm rate and misdetection rate, respectively. Although the actual achievable false alarm and misdetection rates could be slightly higher than  $\alpha$  and  $\beta$  due to approximations and assumptions [45], [46], the real implementation can still refer to  $\alpha$  and  $\beta$  to control the actual performance.

### B. Average Detection Delay Analysis

The aim of SPRT is to achieve the desired false alarm and misdetection rates with the minimal number of detection rounds, which stands for detection delay. The expected number of detection rounds is computed according to [17]:

$$\mathbb{E}[\Lambda_T] = \mathbb{E}[T] \times \mathbb{E}[\lambda_t]. \quad (21)$$

First, we derive the expectation of  $\Lambda_T$  in normal cases, namely, under hypothesis  $\mathcal{H}_1$ . According to (19),  $\mathcal{H}_1$  is accepted when  $\Lambda_T$  reaches the threshold  $\eta_1$ , otherwise  $\mathcal{H}_2$  is accepted (i.e., false alarm). Thus,  $\Lambda_T$  reaches the threshold  $\eta_0$  with the probability of false alarm rate  $\alpha$  and reaches the threshold  $\eta_1$  with probability  $(1-\alpha)$ . Then, according to Eq. (20), we derive the expectation of  $\Lambda_T$  under  $\mathcal{H}_1$ :

$$\mathbb{E}[\Lambda_T | \mathcal{H}_1] = (1-\alpha) \ln \frac{1-\alpha}{\beta} + \alpha \ln \frac{\alpha}{1-\beta}. \quad (22)$$

Similarly, we derive the expectation of  $\Lambda_T$  under  $\mathcal{H}_0$ :

$$\mathbb{E}[\Lambda_T | \mathcal{H}_0] = \beta \ln \frac{1-\alpha}{\beta} + (1-\beta) \ln \frac{\alpha}{1-\beta}. \quad (23)$$

Next, according to Eq. (15), the expectation of  $\lambda_t$  under  $\mathcal{H}_k$  can be expressed as:

$$\mathbb{E}[\lambda_t | \mathcal{H}_k] = \frac{(\mu_1 - \mu_0) \mathbb{E}[\sum_{i_t=1}^{n_t} r_{i_t}^k] + \frac{1}{2} \mathbb{E}[n_t (\mu_0^2 - \mu_1^2)]}{\sigma_0^2}, \quad (24)$$

where  $r_{i_t}^k$  is RSRP from the FAP we are detecting under hypothesis  $\mathcal{H}_k$ .

According to Eqs. (22) (23) and (24), we derive the average detection rounds in normal cases:

$$\mathbb{E}[T | \mathcal{H}_1] = \frac{\sigma_0^2 (1-\alpha) \ln \frac{1-\alpha}{\beta} + \sigma_0^2 \alpha \ln \frac{\alpha}{1-\beta}}{(\mu_1 - \mu_0) \mathbb{E}[\sum_{i_t=1}^{n_t} r_{i_t}^1] + \frac{1}{2} \mathbb{E}[n_t (\mu_0^2 - \mu_1^2)]}, \quad (25)$$

and the average detection rounds in outage cases:

$$\mathbb{E}[T | \mathcal{H}_0] = \frac{\sigma_0^2 \beta \ln \frac{1-\alpha}{\beta} + \sigma_0^2 (1-\beta) \ln \frac{\alpha}{1-\beta}}{(\mu_1 - \mu_0) \mathbb{E}[\sum_{i_t=1}^{n_t} r_{i_t}^0] + \frac{1}{2} \mathbb{E}[n_t (\mu_0^2 - \mu_1^2)]}. \quad (26)$$

To further analyze the impacts of cooperation range, FAP transmission power, and user density, we need to derive the expectation of the sum of test statistics  $\mathbb{E}[\sum_{i_t=1}^{n_t} r_{i_t}^k]$ , which, however, has no closed-form expression. Thus, we approximate the test statistics as follows.

We first approximate  $\mathbb{E}[\sum_{i_t=1}^{n_t} r_{i_t}^1]$ . Note that test statistics follow the Gaussian distribution as described in Eq. (2). The expected sum of test statistics under  $\mathcal{H}_1$  can be written as:

$$\mathbb{E} \left[ \sum_{i_t=1}^{n_t} r_{i_t}^1 \right] = \mathbb{E} \left[ \sum_{i_t=1}^{n_t} r_{i_t} \mathcal{N}(P_{i_t} + N_o, \sigma_0^2) \right], \quad (27)$$

where  $P_{i_t}$  is the received signal strength from the FAP we are detecting. In practice, the measurement error (i.e.,  $\sigma_0^2$ ) is much smaller than RSRP. Thus, we can approximate Eq. (27) as follows:

$$\begin{aligned} \mathbb{E} \left[ \sum_{i_t=1}^{n_t} r_{i_t}^1 \right] &\approx \mathbb{E} \left[ \sum_{i_t=1}^{n_t} P_{i_t} \right] + \mathbb{E} \left[ \sum_{i_t=1}^{n_t} N_o \right] \\ &= P_o \mathbb{E} \left[ \sum_{i_t=1}^{n_t} \left( \frac{d_o}{d_{i_t}} \right)^a e^{X_{i_t}} e^{Y_{i_t}} \right] + N_o \mathbb{E}[n_t] \\ &= P_o \mathbb{E} \left[ \sum_{i_t=1}^{n_t} \left( \frac{d_o}{d_{i_t}} \right)^a \right] \mathbb{E}[e^X] \mathbb{E}[e^Y] + N_o \mathbb{E}[n_t], \end{aligned} \quad (28)$$

where  $P_o$  is FAP's transmission power in normal cases,  $\left(\frac{d_o}{d_{i_t}}\right)^a$  the user  $i$ 's channel gain from path loss at time  $t$ ,  $e^X$  and  $e^Y$  the shadow fading factor and multi-path fading factor, respectively. According to [47], the sum of interference of transmitters with a Poisson distribution to a receiver can be approximated as a log-normal distribution. Correspondingly, we can approximate the sum of the received FAP signal

strengths at users with Poisson distribution as a log-normal distribution in a similar way. Thus, we have:

$$\mathbb{E} \left[ \sum_{i_t=1}^{n_t} \left( \frac{d_o}{d_{i_t}} \right)^a \right] \sim \text{Log-}\mathcal{N}(\mu_m, \sigma_m^2), \quad (29)$$

where  $\mu_m$  and  $\sigma_m^2$  are given by [47]:

$$\mu_m = \frac{1}{2} \ln \left( \frac{m_1^4}{m_1^2 + m_2} \right) \text{ and } \sigma_m^2 = \ln \left( \frac{m_1^2 + m_2}{m_1^2} \right), \quad (30)$$

where  $m_k$  ( $k = 1, 2$ ) is the  $k$ th cumulant of  $\sum_{i_t=1}^{n_t} \left( \frac{d_o}{d_{i_t}} \right)^a$  given as:

$$m_k = \frac{2\rho\pi d_o^{ka}}{ka-2} \left( \frac{1}{\epsilon^{ka-2}} - \frac{1}{R^{ka-2}} \right), \quad (31)$$

where  $\rho$  is the user density,  $\epsilon$  the minimum separation between a user and an FAP, and  $R$  the cooperation range. Only users within  $R$  will report their RSRP statistics to the MBS. In femtocell networks, we have  $ka-2 > 0$  and  $\epsilon \ll R$ . Thus,  $m_k$  can be approximated as:

$$m_k \approx \frac{2\rho\pi d_o^{ka}}{(ka-2)\epsilon^{ka-2}}. \quad (32)$$

By far, we have derived all the expectations that are needed to compute the sum of test statistics, i.e.,  $\mathbb{E}[\sum_{i_t=1}^{n_t} \left( \frac{d_o}{d_{i_t}} \right)^a] = e^{\mu_m + \frac{1}{2}\sigma_m}$ ,  $\mathbb{E}[e^{-X}] = e^{\frac{1}{2}\sigma}$  and  $\mathbb{E}[e^Y] = 1$ . For the average number of test statistics within cooperation range  $n_t$ , since user follow Poisson distribution, we have  $\mathbb{E}[n_t] = \rho\pi R^2$ .

Based on all the above analysis, we finally have  $\mathbb{E}[\lambda|\mathcal{H}_1]$  to be approximated as:

$$\mathbb{E}[\lambda|\mathcal{H}_1] \approx \frac{(\mu_1 - \mu_0)\rho\pi}{\sigma_o^2} \times \left( \left( N_o - \frac{\mu_1 + \mu_0}{2} \right) R^2 + \frac{2P_o d_o^a e^{\frac{1}{2}\sigma^2}}{(a-2)\epsilon^{a-2}} \right).$$

Then, we derive  $\mathbb{E}[\lambda|\mathcal{H}_0]$  as follows. According to (2),  $\mathbb{E}[\sum_{i_t=1}^{n_t} r_{i_t}^1]$  can be expressed as:

$$\mathbb{E} \left[ \sum_{i_t=1}^{n_t} r_{i_t}^0 \right] = \mathbb{E} \left[ \sum_{i_t=1}^{n_t} r_{i_t} \mathcal{N}(N_o, \sigma_o^2) \right] = N_o \rho \pi R^2. \quad (33)$$

Similarly, we derive  $\mathbb{E}[\lambda|\mathcal{H}_0]$  as:

$$\mathbb{E}[\lambda|\mathcal{H}_0] = \frac{(N_o - \frac{\mu_1 + \mu_0}{2})(\mu_1 - \mu_0)\rho\pi R^2}{\sigma_o^2}. \quad (34)$$

Finally, the expected detection delay under  $\mathcal{H}_1$  and  $\mathcal{H}_0$  can be derived by substituting (33) into (25) and substituting (34) into (26), respectively.

$$\mathbb{E}[T|\mathcal{H}_1] = \frac{\sigma_o^2(1-\alpha) \ln \frac{1-\alpha}{\beta} + \sigma_o^2 \alpha \ln \frac{\alpha}{1-\beta}}{(\mu_1 - \mu_0)\rho\pi \left( \left( N_o - \frac{\mu_1 + \mu_0}{2} \right) R^2 + \frac{2P_o d_o^a e^{\frac{1}{2}\sigma^2}}{(a-2)\epsilon^{a-2}} \right)}, \quad (35)$$

$$\mathbb{E}[T|\mathcal{H}_0] = \frac{\sigma_o^2 \beta \ln \frac{1-\alpha}{\beta} + \sigma_o^2 (1-\beta) \ln \frac{\alpha}{1-\beta}}{\left( N_o - \frac{\mu_1 + \mu_0}{2} \right) (\mu_1 - \mu_0)\rho\pi R^2}. \quad (36)$$

Since  $\alpha$  and  $\beta$  are predefined, we have the following observation based on Eq. (36):

**Proposition 1.** *The average outage detection delay is inversely proportional to the user density and the cooperation area (i.e.  $\pi R^2$ ), but is independent of the FAP's transmission power.*

## VII. NUMERICAL RESULTS

In this section, we demonstrate the performance of COD, and the impacts of some system parameters on the detection accuracy and delay with simulation results.

### A. Simulation Setup

We consider a two-tier cellular network comprised of multiple femtocells overlaid on a macrocell. Femtocells are distributed randomly within an area of 1000 m  $\times$  1000 m. All FAPs operate at the carrier frequency of 2.5 GHz with 5 MHz channel bandwidth [44]. Femtocell users are distributed randomly within the same area, and are associated with the FAP with the strongest RSRP. Users send their RSRP reports every 0.1 s. Each femtocell user moves according to the random waypoint mobility model [48] within the range of the network area. Each user moves with speed interval of [0,10] m/s, pause time interval of [0,1] s, and walk interval of [2,6] s. The propagation model is determined based on the ITU and COST231 model which are described in [49], [50]. The transmission powers of FAPs are set according to a self-configuring power control scheme [21]. The misdetection rate and false alarm rate parameters  $\alpha = \beta = 0.01$ . Unless explicitly otherwise stated, the numbers of FAPs and users are 100 and 1000, respectively, cooperation range  $R = 600$  m, and the standard deviation of the shadow fading dB-spread  $\sigma_{dB} = 8$  dB [44], where  $\sigma_{dB} = 10\sigma/\ln(10)$ . The simulation results are the average results from 5000 randomly generated network topologies.

To demonstrate the merits of the proposed statistic correlation based architecture, we compare COD with the commonly used maximum likelihood ratio based approach [51] referred to as MAJ. In MAJ, each user associated with the femtocell in normal state collects RSRP statistics, decides a binary hypothesis problem based on the maximum likelihood ratio, and reports the binary decision directly to the MBS. Then, the MBS makes the decision by majority vote. For a fair comparison, we enhance MAJ by collecting test statistics of the same number of detection rounds as with COD. Thus, both schemes have the same detection delay. To show the performance gain from spatial correlations, we also compare COD with distributed and centralized schemes, both of which adopt the same detection techniques as used in COD but exploits different spatial diversities: the distributed scheme detects outages based on RSRPs collected within each femtocells, while then centralized scheme detects outages by collecting all RSRPs within a macrocell.

### B. Overall Performance

Fig. 3a, Fig. 3b, and Fig. 3c illustrate the overall performance of COD, i.e., average overhead, detection accuracy

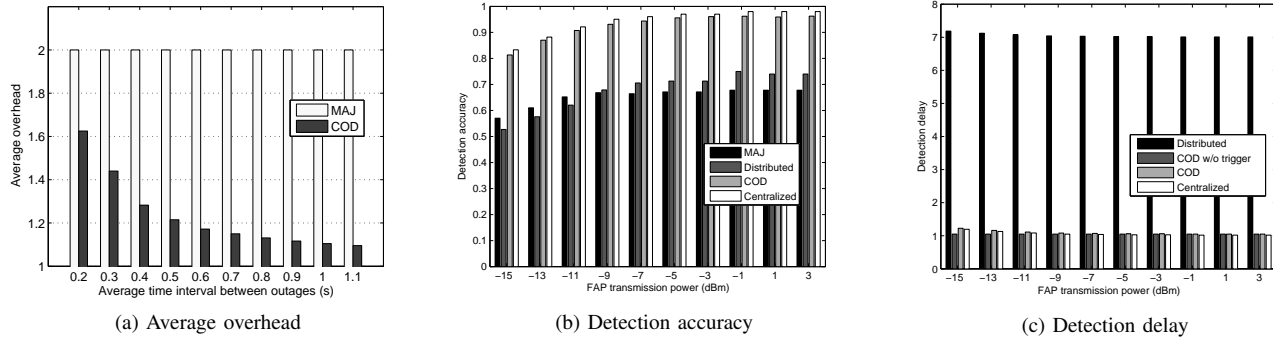


Fig. 3: Overall performance

and detection delay. Average overhead is defined to be the overall number of statistic reports transmitted in each detection round divided by the number of users. Detection accuracy is defined to be the probability of correctly detecting an outaged femtocell. Note that we do not show the false alarm rate in the figures since it is less than 0.001 in all cases, which is much higher than the misdetection rate. Detection delay is defined as the number of detection rounds. In Fig. 3b and Fig. 3c, we set uniform transmission power for FAPs to evaluate the performance of COD under different transmission power levels.

Fig. 3a shows that the average overhead of COD is smaller than MAJ when varying the average time interval between outages. The merit of COD comes from the distributed trigger mechanism. The average overhead of COD decreases when the average time interval between outages increases, namely, the frequency of outages decreases. This is because the lower frequency of outages means that there are fewer chances of COD triggering the cooperative detection stage, which requires more overhead than the trigger stage. Note that in practice, the frequency of outages can be much lower (i.e., larger time interval), in which case the merits of COD are more obvious.

Fig. 3b depicts the detection accuracy for various FAP power levels, and it is shown that COD outperforms MAJ in detection accuracy by more than 20% in all cases demonstrated. We also see that the proposed scheme achieves similar accuracy compared to the centralized scheme, and outperforms the distributed scheme over 20% in all cases. This is because COD exploits spatial correlations by collaborative filtering and data fusion to obtain more information for the final decision, while MAJ simply aggregates statistics by majority vote. We observe that both COD and MAJ detect outaged femtocells with higher accuracy as the FAP power increases. This is because when FAP transmission power increases, the gap between the RSRP statistics in normal cases and RSRP statistics in outage cases is larger, making it easier to differentiate these two cases.

From Fig. 3c, we see that COD enjoys similar detection delay compared with the centralized scheme, and can detect outage within two detection rounds in all cases in the figure. Fig. 3c also indicates that the difference in the detection delays of COD without trigger stage and COD approaches zero when FAP transmission power increases. The reason is that as the

FAP power gets larger, it is easier to differentiate outage cases from normal cases, the probability of immediately triggering the detection stage is higher. We also observe that the detection delay of COD without trigger stage is independent of the FAP transmission power, which matches our analytical results in Proposition 1.

## VIII. CONCLUSIONS

This paper proposes COD, a cooperative detection architecture to detect femtocell outages. COD considers the challenges caused by the distinct features of the two-tier femto-macro networks, including dense deployments, vertical handover, and sparse user statistics. To resolve these issues, COD leverages collaborative filtering and sequential hypothesis detection to exploit the spatial and temporal correlations among RSRP statistics across different femtocells. Our evaluations show that our cooperative detection largely reduces communication overhead and achieves higher detection accuracy than the existing approach under the same delay condition. Both analytical and numerical results validate the correlation-based cooperative detection architecture, which can be used as a general framework for future femtocell outage detection scheme design. This paper also provides some guidelines through theoretical analyses and numerical evaluations that the detection performance is inversely proportional to the user density and the cooperation area, but is independent of the FAP's transmission power.

### APPENDIX A PROOF OF LEMMA 1

The subproblem (7) should be solved in two cases, that is,  $\mathbf{V}_{\cdot k} = 0$  and  $\mathbf{V}_{\cdot k} \neq 0$ . If  $\mathbf{V}_{\cdot k} = 0$ , the subproblem (7) has an infinite number of solutions. Therefore, the  $k$ th column of both  $\mathbf{U}$  and  $\mathbf{V}$  should be removed in the remaining computation. If  $\mathbf{V}_{\cdot k} \neq 0$ , according to [39], the subproblem (7) has a closed-form solution

$$\mathbf{U}_{\cdot k} = \frac{\prod_+(\mathbf{E}_k \mathbf{V}_{\cdot k})}{\|\mathbf{V}_{\cdot k}\|_2^2}. \quad (37)$$

Similarly, the subproblem (8) should be considered in two cases, that is,  $\mathbf{U}_{\cdot k} = 0$  and  $\mathbf{U}_{\cdot k} \neq 0$ . If  $\mathbf{U}_{\cdot k} = 0$ , the  $k$ th column of both  $\mathbf{U}$  and  $\mathbf{V}$  does not take part in the remaining computation and should be taken off. If  $\mathbf{U}_{\cdot k} \neq 0$ , below we

show how to solve (8) in an analytic formulation though it is not as direct as (37).

We solved the constrained optimization (8) by using the Lagrangian multiplier method [52]. The Lagrangian function of (8) is

$$\mathcal{L} = \|\mathbf{E}_k - \mathbf{U}_{\cdot k} \mathbf{V}_{\cdot k}^\top\|_F^2 + \lambda \mathbf{V}_{\cdot k}^\top \mathbf{L} \mathbf{V}_{\cdot k} - \langle \mathbf{V}_{\cdot k}, \lambda \rangle, \quad (38)$$

where  $\gamma$  is the Lagrangian multiplier for the constraint  $\mathbf{V}_{\cdot k} \geq 0$ . Based on the *Karush-Kuhn-Tucker* (K.K.T.) conditions, the solution of [39] satisfies

$$\begin{cases} \mathbf{V}_{\cdot k} \geq 0, \gamma \geq 0, \\ \frac{\partial \mathcal{L}}{\partial \mathbf{V}_{\cdot k}} = -\mathbf{E}_k^\top \mathbf{U}_{\cdot k} + (\|\mathbf{U}_{\cdot k}\|_2^2 \mathbf{I} + \lambda \mathbf{L}) \mathbf{V}_{\cdot k} - \gamma = 0 \\ \gamma \mathbf{V}_{\cdot k} = \mathbf{0} \end{cases} \quad (39)$$

where  $\mathbf{I} \in \mathbb{R}^{n \times n}$  is an identity matrix. With simple algebra, based on (14), we update columns of  $V$  as follows:

$$\mathbf{V}_{\cdot k} = \prod_{+} ((\|\mathbf{U}_{\cdot k}\|_2^2 \mathbf{I} + \lambda \mathbf{L})^{-1} \mathbf{E}_k^\top \mathbf{U}_{\cdot k}). \quad (40)$$

By updating columns of  $U$  and  $V$  alternatively with (37) and (40), respectively, until convergence, which solves Problem (6).

#### APPENDIX B PROOF OF THEOREM 1

Note that the feasible sets of  $\mathbf{U}_{\cdot k}$  and  $\mathbf{V}_{\cdot k}$  are  $\Omega_k^U \subset \mathbb{R}_+^m$  and  $\Omega_k^V \subset \mathbb{R}_+^n$ . According to [53], since  $\hat{\mathbf{R}}$  is bounded, we can set an upper bound for  $\Omega_k^U$  and  $\Omega_k^V$  and can thus consider them as closed convex sets.

Therefore, the GNMF problem can be written as a bound-constrained optimization problem

$$\min_{[\mathbf{U}, \mathbf{V}] \in \Omega} \left\| \hat{\mathbf{R}} - \sum_{k=1}^d \mathbf{U}_{\cdot k} \mathbf{V}_{\cdot k}^\top \right\|_F^2 + \lambda \sum_{k=1}^r \mathbf{V}_{\cdot k}^\top \mathbf{L} \mathbf{V}_{\cdot k}, \quad (41)$$

where  $\Omega = \prod_{k=1}^d \Omega_k^U \times \prod_{k=1}^d \Omega_k^V$  is a Cartesian product of closed convex sets. Since the objective function of (41) is continuously differentiable over  $\Omega$  and the proposed algorithm updates the  $k$ th column of  $\mathbf{U}$  and  $\mathbf{V}$  with the optimal solutions of (9) and (10), every limit point generated by (9) and (10) is a stationary point [52].

For completeness, we must consider cases when either  $\mathbf{U}_{\cdot k}$  or  $\mathbf{V}_{\cdot k}$  is zero. As mentioned above, such columns should be removed without changing the value of the objective function (41). Therefore, these columns do not destroy the theoretic analysis, which completes the proof.

#### APPENDIX C PROOF OF THEOREM 2

Let  $\mathcal{E}(\hat{\mathbf{R}}, \mathbf{U} \mathbf{V}^\top)$  denote the approximation error with respect to  $\hat{\mathbf{R}}$ , i.e.,  $\mathcal{E}(\hat{\mathbf{R}}, \mathbf{U} \mathbf{V}^\top) \triangleq \frac{1}{mn} \sum_{i=1}^m \sum_{k=1}^n |\hat{R}_{i,k} - \sum_{l=1}^d U_{i,l} V_{l,k}|$ . We first derive the upper bound for  $\mathcal{E}(\hat{\mathbf{R}}, \mathbf{U} \mathbf{V}^\top)$ .

We denote the singular values of  $\hat{\mathbf{R}}$  as  $\{o_1, \dots, o_d\}$ . Let  $\mathbf{\Sigma}$  be a diagonal matrix where the  $l$ th element on the diagonal is  $o_l$ , we have

$$|\mathbf{U} \mathbf{V}^\top - \mathbf{U} \mathbf{\Sigma} \mathbf{V}^\top| = \sum_{i=1}^m \sum_{k=1}^n \left| \sum_{l=1}^d (1 - o_l) V_{i,l} U_{k,l} \right|. \quad (42)$$

Similarly, we have

$$|\hat{\mathbf{R}} - \mathbf{U} \mathbf{\Sigma} \mathbf{V}^\top| = \sum_{i=1}^m \sum_{k=1}^n \left| \hat{R}_{i,k} - \sum_{l=1}^d o_l V_{i,l} U_{k,l} \right|. \quad (43)$$

Then, we can derive

$$\mathcal{E}(\hat{\mathbf{R}}, \mathbf{U} \mathbf{V}^\top) \leq \sum_{i=1}^m \sum_{k=1}^n \left( \sqrt{\sum_{l=d+1}^{\text{rank}(\hat{\mathbf{R}})} o_l^2 + \sum_{l=1}^d |1 - o_l| V_{i,l} U_{k,l}} \right). \quad (44)$$

Now we develop the upper bound for  $\mathcal{E}(\mathbf{P}, \mathbf{U} \mathbf{V}^\top)$ . Recall that  $\hat{\mathbf{R}} = \mathbf{P} + \mathbf{X}$ , where  $\mathbf{X}$  is the shadow fading matrix with each element following independent Gaussian distribution  $\mathcal{N}(0, \sigma)$ . Then, we have

$$\begin{aligned} & \mathcal{E}(\mathbf{P}, \mathbf{U} \mathbf{V}^\top) - \mathcal{E}(\hat{\mathbf{R}}, \mathbf{U} \mathbf{V}^\top) \\ &= \frac{1}{mn} \sum_{i=1}^m \sum_{k=1}^n \left( \left| P_{i,k} - \sum_{l=1}^d U_{i,l} V_{l,k} \right| \right. \\ & \quad \left. - \left| P_{i,k} + X_{i,k} - \sum_{l=1}^d U_{i,l} V_{l,k} \right| \right) \\ & \leq \frac{1}{mn} \sum_{i=1}^m \sum_{k=1}^n |X_{i,k}| = \frac{1}{mn} \sum_{i=1}^m |X_i|. \end{aligned} \quad (45)$$

Let  $Y = \frac{1}{mn} \sum_{i=1}^m |X_i|$ . By incorporating the exponential Chebyshev's inequality,  $\forall t > 0$ ,

$$\begin{aligned} \Pr[Y \geq \varepsilon] & \leq e^{-t\varepsilon} \mathbb{E}[e^{tY}] = e^{-t\varepsilon} \prod_{i=1}^{mn} \mathbb{E}[e^{\frac{t}{mn} |X_i|}] \\ & = e^{-t\varepsilon} \left( \frac{2}{\sigma \sqrt{2\pi}} \int_0^{+\infty} e^{\frac{t}{mn} x} e^{-\frac{x^2}{2\sigma^2}} dx \right)^{mn} \\ & = e^{-t\varepsilon} \left( 2e^{\frac{\sigma^4 t^2}{2(mn)^2}} Q\left(-\frac{t\sigma^2}{mn}\right) \right)^{mn} \\ & = e^{\frac{\sigma^2 t^2}{2mn} - \varepsilon t} (2 - 2Q\left(\frac{t\sigma^2}{mn}\right))^{mn}, \end{aligned} \quad (46)$$

where  $Q(\cdot)$  signifies the Q-function. To derive a tight bound, we set  $t = \frac{mn\varepsilon}{\sigma^2}$  to minimize the exponential term in the right hand side of the above inequality. Therefore, we have

$$\Pr[Y \geq \varepsilon] \leq e^{-\frac{mn\varepsilon^2}{2\sigma^2}} (2 - 2Q(\varepsilon))^{mn}. \quad (47)$$

Let  $\delta = e^{-\frac{mn\varepsilon^2}{2\sigma^2}} (2 - 2Q(\varepsilon))^{mn}$ , we have  $\Pr[Y < \varepsilon] \geq 1 - \delta$ . By combining Eq. (44), we prove the theorem.

## REFERENCES

- [1] “Telecommunication management; self-organizing networks (SON) policy network resource model (NRM) integration reference point (IRP); information service (IS).” 3GPP TS 32.522, Rel. 9, Mar. 2010.
- [2] “Telecommunication management; self-organizing networks (SON); self-healing concepts and requirements.” 3GPP TS 32.541, Rel. 10, Mar. 2011.
- [3] R. Combes, Z. Altman, and E. Altman, “Self-organization in wireless networks: A flow-level perspective,” in *Proc. IEEE INFOCOM*, Mar. 2012.
- [4] A. Stolyar and H. Viswanathan, “Self-organizing dynamic fractional frequency reuse for best-effort traffic through distributed inter-cell coordination,” in *Proc. IEEE INFOCOM*, Apr. 2009.
- [5] M. Amirijoo *et al.*, “Cell outage management in lte networks.” COST 2100 TD(09)941, Sep. 2009.
- [6] “Self-organizing networks, NEC’s proposals for next-generalization radio network management.” NEC White Paper, 2009.
- [7] C. Mueller, M. Kaschub, C. Blankenhorn, and S. Wanke, “A cell outage detection algorithm using neighbor cell list reports,” *International Workshop on Self-Organizing Systems*, pp. 218–229, 2008.
- [8] R. Khanfer *et al.*, “Automated diagnosis for UMTS networks using bayesian network approach,” *IEEE Trans. Veh. Technol.*, vol. 57, no. 4, pp. 2451–2461, Jul. 2008.
- [9] Y. Ma, M. Peng, W. Xue, and X. Ji, “A dynamic affinity propagation clustering algorithm for cell outage detection in self-healing networks,” in *Proc. IEEE WCNC*, 2013, pp. 2266–2270.
- [10] “3G Home NodeB (HNB) study item.” 3GPP TR 25.820, Mar. 2008.
- [11] A. Damnjanovic, J. Montojo, Y. Wei, T. Ji, T. Luo, M. Vajapeyam, T. Yoo, O. Song, and D. Malladi, “A survey on 3gpp heterogeneous networks,” *IEEE Wireless Commun.*, vol. 18, no. 3, pp. 10–21, 2011.
- [12] V. Chandrasekhar, J. Andrews, and A. Gatherer, “Femtocell networks: a survey,” *IEEE Commun. Magazine*, vol. 46, no. 9, pp. 59–67, Sep. 2008.
- [13] “Evolved Universal Terrestrial Radio Access Network (E-UTRAN); physical layer - measurements.” 3GPP TS 36.214, Dec. 2008.
- [14] R. Chandra, V. N. Padmanabhan, and M. Zhang, “Wifiprofiler: cooperative diagnosis in wireless LANs,” in *Proc. ACM MobiSys*, 2006.
- [15] A. Adya, P. Bahl, R. Chandra, and L. Qiu, “Architecture and techniques for diagnosing faults in ieee 802.11 infrastructure networks,” in *Proc. ACM MobiCom*, 2004.
- [16] D. Goldberg, D. Nichols, B. M. Oki, and D. Terry, “Using collaborative filtering to weave an information tapestry,” *Commun. ACM*, vol. 35, no. 12, pp. 61–70, Dec. 1992.
- [17] A. Wald, “Sequential tests of statistical hypotheses,” *Ann. Math. Statist.*, vol. 16, no. 2, pp. 117–186, 1945.
- [18] M. Peng, Z. Ding, Y. Zhou, and Y. Li, “Advanced self-organizing technologies over distributed wireless networks,” *International Journal of Distributed Sensor Networks*, vol. 2012, 2012.
- [19] O. G. Aliu, A. Imran, M. A. Imran, and B. Evans, “A survey of self organisation in future cellular networks,” *IEEE Commun. Surveys & Tutorials*, vol. 15, no. 1, pp. 336–361, 2013.
- [20] M. Peng, D. Liang, Y. Wei, J. Li, and H.-H. Chen, “Self-configuration and self-optimization in lte-advanced heterogeneous networks,” *IEEE Commun. Mag.*, vol. 51, no. 5, pp. 36–45, 2013.
- [21] D. López-Pérez, X. Chu, A. V. Vasilakos, and H. Claussen, “On distributed and coordinated resource allocation for interference mitigation in self-organizing lte networks,” *IEEE/ACM Trans. Netw.*, vol. 21, no. 4, pp. 1145–1158, 2013.
- [22] J.-H. Yun and K. G. Shin, “Adaptive interference management of ofdma femtocells for co-channel deployment,” *IEEE J. Sel. Area Commun.*, vol. 29, no. 6, pp. 1225–1241, 2011.
- [23] R. Barco, P. Lazaro, and P. Munoz, “A unified framework for self-healing in wireless networks,” *IEEE Commun. Mag.*, vol. 50, no. 12, pp. 134–142, 2012.
- [24] M. Amirijoo, L. Jorgueski, R. Litjens, and L. Schmelz, “Cell outage compensation in lte networks: Algorithms and performance assessment,” in *Proc. IEEE VTC*, 2011, pp. 1–5.
- [25] L. Xia, W. Li, H. Zhang, and Z. Wang, “A cell outage compensation mechanism in self-organizing ran,” in *WiCOM*, 2011, pp. 1–4.
- [26] W. Wang, J. Zhang, and Q. Zhang, “Transfer learning based diagnosis for configuration troubleshooting in self-organizing femtocell networks,” in *Proc. IEEE GLOBECOM*, 2012.
- [27] J. Turkka, F. Chernogorov, K. Brigatti, T. Ristaniemi, and J. Lempinen, “An approach for network outage detection from drive-testing databases,” *Journal of Computer Networks and Communications*, vol. 2012, 2012.
- [28] “Evolved universal terrestrial radio access network (e-utran); self-configuring and self-optimizing network use cases and solutions.” 3GPP TR 36.902, Rel. 11, Feb. 2012.
- [29] “Universal terrestrial radio access (utra) and evolved universal terrestrial radio access (e-utra); radio measurement collection for minimization of drive tests (mdt); overall description; stage 2.” 3GPP TS 37.320, Rel. 11, Jun. 2011.
- [30] W. Wang, J. Zhang, and Q. Zhang, “Transfer learning based diagnosis for configuration troubleshooting in self-organizing femtocell networks,” in *Proc. IEEE GLOBECOM*, Dec. 2011.
- [31] R. Chen, J.-M. Park, and K. Bian, “Robust distributed spectrum sensing in cognitive radio networks,” in *Proc. IEEE INFOCOM*, Apr. 2008.
- [32] A. Min, X. Zhang, and K. Shin, “Spatio-temporal fusion for small-scale primary detection in cognitive radio networks,” in *Proc. IEEE INFOCOM*, Mar. 2010.
- [33] V. Erceg *et al.*, “An empirically based path loss model for wireless channels in suburban environments,” *IEEE J. Sel. Areas Commun.*, vol. 17, no. 7, pp. 1205–1211, 1999.
- [34] S. Shellhammer *et al.*, “Performance of power detector sensors of DTV signals in IEEE 802.22 WRANs,” in *Proc. ACM TAPAS*, 2006.
- [35] D. Fan, Z. Feng, L. Tan, V. Le, and J. Song, “Distributed self-healing for reconfigurable WLANs,” in *Proc. IEEE WCNC*, Apr. 2010.
- [36] X. Chen, J. Huang, and H. Li, “Adaptive channel recommendation for dynamic spectrum access,” in *Proc. IEEE DySPAN*, May 2011.
- [37] Y. Koren, “Factorization meets the neighborhood: a multifaceted collaborative filtering model,” in *Proc. ACM SIGKDD*, 2008.
- [38] J. Wang and D. Katabi, “Dude, where’s my card? rfid positioning that works with multipath and non-line of sight,” in *Proc. ACM SIGCOMM*, Aug. 2013.
- [39] D. Cai, X. He, X. Wu, and J. Han, “Non-negative matrix factorization on manifold,” in *Proc. IEEE ICDM*, Dec. 2008.
- [40] D. Cai, X. He, J. Han, and T. S. Huang, “Graph regularized nonnegative matrix factorization for data representation,” *IEEE Trans. Pattern Anal. Mach. Intell.*, vol. 33, no. 8, pp. 1548–1560, 2011.
- [41] N. D. Ho, P. Van Dooren, and V. D. Blondel, “Descent methods for nonnegative matrix factorization,” in *Numerical Linear Algebra in Signals, Systems and Control*. Springer, 2011.
- [42] A. Cichocki, R. Zdunek, and S.-i. Amari, “Hierarchical als algorithms for nonnegative matrix and 3d tensor factorization,” in *Independent Component Analysis and Signal Separation*. Springer, 2007.
- [43] N. Srebro, N. Alon, and T. Jaakkola, “Generalization error bounds for collaborative prediction with low-rank matrices,” in *Proc. NIPS*, Dec. 2004.
- [44] J.-H. Yun and K. G. Shin, “Ctrl: a self-organizing femtocell management architecture for co-channel deployment,” in *Proc. ACM MobiCom*, Sep. 2010.
- [45] P. Varshney and C. Burrus, *Distributed detection and data fusion*. Springer Verlag, 1997.
- [46] A. W. Min, K. G. Shin, and X. Hu, “Secure cooperative sensing in ieee 802.22 wrans using shadow fading correlation,” *IEEE Trans. Mobile Comput.*, vol. 10, no. 10, pp. 1434–1447, 2011.
- [47] R. Menon, R. Buehrer, and J. Reed, “On the impact of dynamic spectrum sharing techniques on legacy radio systems,” *IEEE Trans. Wireless Commun.*, vol. 7, no. 11, pp. 4198–4207, Nov. 2008.
- [48] C. Bettstetter, G. Resta, and P. Santi, “The node distribution of the random waypoint mobility model for wireless ad hoc networks,” *IEEE Trans. Mobile Computing*, vol. 2, no. 3, pp. 257–269, Jul.-Sep. 2003.
- [49] “Guidelines for evaluation of radio transmission technologies for imt-2000,” *ITU-R Rec M.1225*, 1997.
- [50] “Digital mobile radio towards future generation systems: Final report,” *COST Action 231*, 1999.
- [51] H. Akaike, “Information theory and an extension of the maximum likelihood principle,” in *Proc. IEEE ISIT*, Jul. 1973.
- [52] D. P. Bertsekas, *Nonlinear programming*. Athena Scientific, 1999.
- [53] C. J. Lin, “Projected gradient methods for nonnegative matrix factorization,” *Neural computation*, vol. 19, no. 10, pp. 2756–2779, 2007.